Received: 11 May 2022 | Revised: 24 June 2022 | Accepted: 5 July 2022

DOI: 10.1002/bio.4326

RESEARCH ARTICLE

LUMINESCENCE WILEY
The Journal of Biological and Chemical Luminescence

A novel nanosponge–hydrogel system-based electrochemiluminescence biosensor for uric acid detection

Wanqing Liu[1,2] | Yixin Nie[1] | Mengmeng Zhang[1,2] | Kefan Yan[1,2] | Mai Wang[1,2] | Yupeng Guo[1,2] | Qiang Ma[1,2]

[1]Department of Analytical Chemistry, College of Chemistry, Jilin University, Changchun, China

[2]National Chemistry Experimental Teaching Demonstration Center, Jilin University, Jilin, Changchun, China

Correspondence
Qiang Ma, National Chemistry Experimental Teaching Demonstration Center, Jilin University, Changchun 130012, Jilin, China.
Email: qma@jlu.edu.cn

Funding information
the science research project in the Education Department of Jilin Province, China; Education Department of Jilin Province, China; National Natural Science Foundation of China, Grant/Award Number: 22174051

Abstract

In this work, a highly efficient electrochemiluminescence (ECL) biosensor was developed based on the nanosponge–hydrogel system for uric acid (UA) detection. First, the nanosponge consisted of polylactic acid glycolic acid (PLGA) nanoparticles immobilized with MoS_2 quantum dots (QDs) and urate oxidase (UAO). The marked loading capability of PLGA nanoparticles enables loading many biomolecules and QDs for the specific recognition of UA. Urate oxidase on the nanosponge can catalyze UA to generate H_2O_2 *in situ*, which further triggers the ECL signal for the MoS_2 QDs. Furthermore, the biocompatible acrylamide-based hydrogel not only effectively retained the functionalities of the chimeric nanosponge–hydrogel, but also provided structural integrity and engineering flexibility on the electrode for ECL sensing applications. In addition, there were many ester groups and amide bonds in the nanosponge–hydrogel structure. Therefore, many electron can be excited in the ECL process due to the large number of lone electron pairs on oxygen and nitrogen atoms. This resulted in a seven-fold ECL enhancement of the MoS_2 QDs. Finally, the nanosponge–hydrogel structure-based ECL biosensor was successfully used in real clinical serum assays. This showed a good analytical performance for UA detection (100–500 μmol/L) with a limit of detection of 20 μmol/L.

KEYWORDS
electrochemiluminescence, hydrogel, MoS_2 QDs, nanosponge, uric acid detection

1 | INTRODUCTION

Uric acid (UA) is the product of purine metabolism under the action of enzymes.[1] For humans, 20% of purine is produced by food and 80% by the body itself. Urate oxidase (UAO) in mammals can break down UA into allantoin. Because there is no UAO in the human body, UA with its high concentration in the blood can accumulate with the formation of UA crystals. UA deposition in the corresponding areas can result in multiple systemic diseases including gout, kidney disease, and diabetes.[2] Therefore, UA detection is necessary for clinical diagnosis. Detection methods mainly include a routine urine examination, the determination of blood uric acid, and the measurement of total UA over a 24 h period.[3] To date, analytical methods and biosensor-related research have made important progress in the detection of UA with high sensitivity, such as through fluorescence assay, capillary electrophoresis, and high-performance liquid chromatography (HPLC). For example, Khajehsharifi et al. developed an orthogonal signal corrected partial least squares method for simultaneous spectrophotometric determination of whey acid, creatinine, and UA.[4] Chu et al. developed a biosensor based on polypyrrole immobilized uricase for UA detection.[5] Jie et al. developed a kinetic method for the determination of UA using the noncatalytic BZ reaction in a nonequilibrium

steady state.[6] Amjadi et al. developed a method based on silver nanoparticle plasma resonance for the determination of UA in human plasma and urine samples.[7] Despite their different advantages, these methods still have some limitations, such as a complex detection process and long detection time. In particular, due to the actual needs of UA tests at the point of care, there is still a challenge to develop highly efficient sensing methods to improve the detection performance of UA.

Electrochemiluminescence (ECL) technology is an important analysis method, it has been widely used in clinical diagnosis and bioanalytical chemistry.[8,9] In the generation process of ECL, the species react on the electrode surface with the high energy electron transfer reactions. The resulted excited states can emit light immediately. ECL has the unique characteristics of low background signals without the excitation source and a simple operation. So, ECL assays can be used in a point of care test with high sensitivity, low detection limit, and wide linear working range. Recently, the gel has acted as a new functional material in the construction of ECL sensors. The gel composites can load ECL luminophores or electrolytes, and expand the potential application of ECL in flexible and portable devices. For example, Chansri et al. reported a simple preparation process for ECL cells based on silica gel-type solvents using a ZnO/TiO_2 nanotubes electrode.[10] Kwon et al. extended the porous ion gel in the production of emissive ECL ionoskins.[11] Shan's group synthesized metal–organic gels using horseradish peroxidase.[12] Metal–organic gels based on the EC platform were used for *in situ* detection of H_2O_2 generated from HeLa cells. However, the gel was just used as a simple carrier in the ECL sensing application. The adsorption ability, structure characteristics, and other functional properties of gels should be further improved.

In this work, an ECL biosensor was designed based on the nanosponge–hydrogel system for uric acid detection (as shown in Scheme 1).[13] The nanosponge consisted of a polylactic acid glycolic acid copolymer (PLGA) nanoparticle core immobilized with MoS_2 QDs and UAO molecules, which worked as an ECL emitter and recognition unit in the sensor, respectively. The environmentally friendly and degradable PLGA was polymerized from two monomers, lactic acid and glycolic acid, which had good biocompatibility, nontoxic, environmental friendliness, high encapsulation, and has been widely used in the pharmacy medical engineering materials and biomedical fields.[14–16] Moreover, PLGA nanoparticles contained many ester functional groups with large numbers of solitary electron pairs. Therefore, the nanosponge-based ECL sensing system provided the marked capabilities of effective adsorption and determination of UA. Furthermore, when the nanosponge was composited in the hydrogel, the adsorption ability was improved largely over that of the separate PLGA nanoparticles. In addition, the ester groups and amide bonds in the nanosponge–hydrogel structure further amplified the ECL intensity of the MoS_2 QDs. Due to the nanosponge–hydrogel structure, UA molecules were absorbed from serum and decomposed using UAO catalysis to generate hydrogen peroxide.[17] Consequently, hydrogen peroxide worked as the co-reactant and reacted with MoS_2 QDs to emit the ECL signal. The detection results demonstrated the advantages of this nanosponge–hydrogel system in the ECL sensor.

2 | EXPERIMENTAL

2.1 | Chemicals and apparatus

PLGA, glutathione (GSH), ammonium molybdate ($[NH_4]_2MoO_4$), tetramethylethylenediamine (TEMED), acrylamide (C_3H_5NO), ammonium persulfate ($NH_4S_2O_8$), polyethylene glycol dimethacrylate (PEGDMA), potassium ferricyanide ($K_3[Fe\ [CN]_6]$), potassium ferrocyanide ($K_4[Fe\ [CN]_6]$), chlorine potassium (KCl), sodium dihydrogen phosphate (NaH_2PO_4), hydrogen diphosphate sodium (Na_2HPO_4), sodium phosphate (Na_3PO_4), UA, uricase (UAO), glycine (Gly), glutamic (Glu), cystine (Cys), urea and glucose (Glu) were obtained from Sinopharm Holdings. All chemicals were used without further purification.

TEM images of MoS_2 QDs were recorded on a JEM-2100F field emission electron microscope at an acceleration voltage of 200 kV.

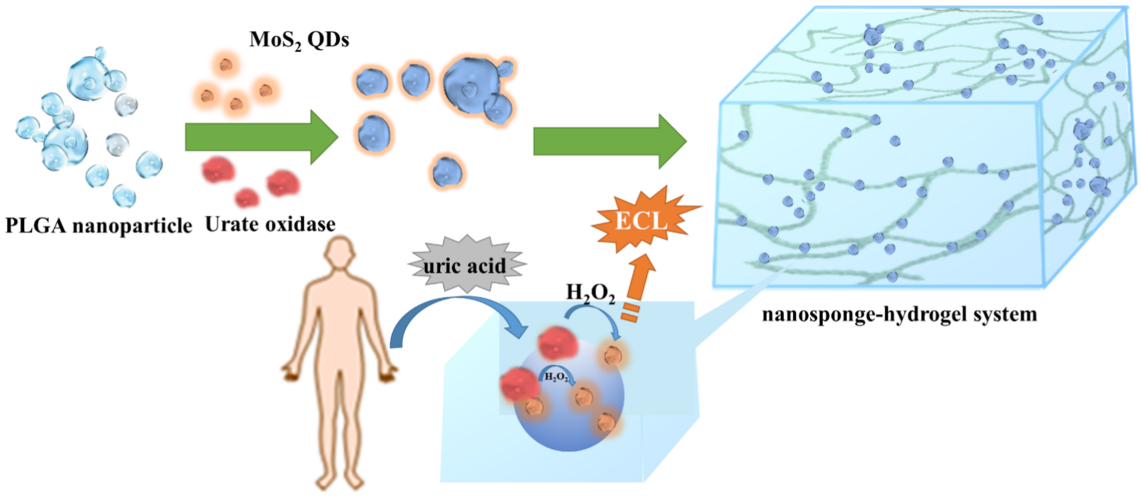

SCHEME 1 Illustration of the nanosponge–hydrogel system-based ECL sensor for UA detection

Scanning electron microscopy (SEM) images of the PLGA and gel patterned structures were recorded on a Hitachi SU8020 field emission scanning electron microscope. Fourier transform infrared spectroscopy (FTIR) and ultraviolet–visible (UV–vis) absorption spectra were obtained on the Thermo Nicolet 360 FTIR spectrometer and a Hitachi UH5300 UV–visible spectrophotometer, respectively. A F-2700 fluorescence spectrophotometer was used to record the fluorescence spectra. The electrochemical data and ECL signals were obtained via a CHI 660B electrochemical workstation, H10682-210 photomultiplier tubes, and the c8855-01 signal recording unit from Hamamatsu Photonics Co. Ltd.

2.2 | Synthesis of MoS_2 QDs

MoS_2 QDs were synthesized using the microwave-assisted solvothermal method. Here, 0.047 g ammonium molybdate tetrahydrate and 0.254 g reduced glutathione were dissolved in 12 ml of ultrapure water. The solution was heated at 180°C under microwave-assisted conditions for 50 min using a programmed process. Then the product was centrifuged for 10 min (10,000 rpm). The yellow supernatant was collected and further dialyzed to obtain MoS_2 QDs.[18] The product was stored at 4°C for the next steps.

2.3 | Synthesis of nanosponge

Here, 100 mg solid PLGA was dissolved in 10 ml acetone for 30 min; 30 ml deionized water was added into the above solution with continuous stirring for 1 h.[13] Then, the solution was heated to 100°C for 30 min. The mixture was centrifuged at 10,000 rpm for 5 min. The obtained PLGA nanoparticles were collected. Next, 20 mg PLGA nanoparticles were added into 0.5 ml MoS_2 QDs. After incubation for 5 min, MoS_2 QDs were adsorbed on the PLGA nanoparticle surface. The PLGA nanoparticles with MoS_2 QDs were centrifuged at 10,000 rpm for 5 min and washed again. Then 10 mg/ml UAO were incubated with the nanoparticles for 10 min. After centrifugation at 10,000 rpm for 5 min they were washed again, the nanosponge was obtained according to the above method.

2.4 | Synthesis of the nanosponge–hydrogel system

Here, 40 mg/ml acrylamide was used as a monomer in the reaction system. Then 1 mg/ml PEGDMA was used as a crosslinking agent; 1 μl TEMED and 2 μl ammonium persulfate were added and mixed. Within 2 min, the prepared gel could be observed.[13] Then, the as-prepared PLGA nanoparticles with a final concentration of 3 mg/ml were added into the gel to obtain the nanosponge–hydrogel system. The nanosponge–hydrogel was dropped onto the electrode surface at room temperature. ECL testing processes were performed in PBS (pH 7.4) with different concentrations of UA.

3 | RESULTS AND DISCUSSION

3.1 | Characterization of MoS_2 QDs

The TEM diagram of MoS_2 QDs is shown in Figure 1a. The morphology of the MoS_2 QDs showed good uniformity and dispersion with an average particle size of 8 nm. The crystal phase of the MoS_2 QDs was investigated using X-ray diffraction (XRD) and shown in Figure 1b. The XRD patterns showed that the MoS_2 QDs had an amorphous structure. Fourier transform infrared (FTIR) spectroscopy of MoS_2 QDs is shown in Figure 1c. The stretching vibrations and bending vibrations of N–H were located at 3240 cm^{-1} and 1630 cm^{-1}, respectively. These indicated that amino groups were present. The stretching vibration and bending vibration of O–H were located at 3100 cm^{-1}. The characteristic peaks at 1743 cm^{-1} were attributed to C=O bonds. The peaks at 1410 cm^{-1} and 1270 cm^{-1}, respectively, corresponded to the stretching vibration of C–N and C–O bonds. The UV–vis absorption spectrum of MoS_2 QDs is recorded in Figure 1d. In the UV absorption spectra, there was a characteristic absorption peak at 310 nm.

ECL intensity and the cyclic voltammetry curve of MoS_2 QDs in PBS (pH 7.4) buffer solution with hydrogen peroxide as co-reactant are shown in Figure 2. It can be seen that the ECL intensity of the MoS_2 QDs is relatively observable with H_2O_2. MoS_2 QDs exhibited strong ECL intensity with the excitation potential at −1.8 V. Photoluminescence spectra in Figure 2c displayed the excitation wavelength-dependent properties of MoS_2 QDs. They emitted the maximum photoluminescence intensity at 340 nm. The photographs of fluorescence in Figure 2d demonstrated that the MoS_2 QDs had strong yellow fluorescence under irradiation from a UV light lamp. The possible ECL mechanisms of MoS_2 QDs are outlined in the following equations:

$$H_2O_2 + e^- \rightarrow \cdot OH + OH^- \quad (1)$$

$$\cdot OH + MoS_2\,QDs + e^- \rightarrow MoS_2\,QDs^* + OH^- \quad (2)$$

$$MoS_2\,QDs^* \rightarrow MoS_2\,QDs + hv \quad (3)$$

3.2 | Characterization of nanosponge–hydrogel system

It can be seen in Figure 3a that the diameter of the PLGA nanoparticles synthesized using an emulsion solution volatilization method was ~180 nm. PLGA nanoparticles had uniform spherical morphology. FTIR spectroscopy of the PLGA nanoparticles is shown in Figure 3b. The stretching vibrations and bending vibrations of O–H bonds are located at 2900 cm^{-1} and 1610 cm^{-1}, respectively. These indicated that hydroxyl groups were present. The characteristic peaks locating at 1750 cm^{-1} were attributed to the C=O bond. Combined with the

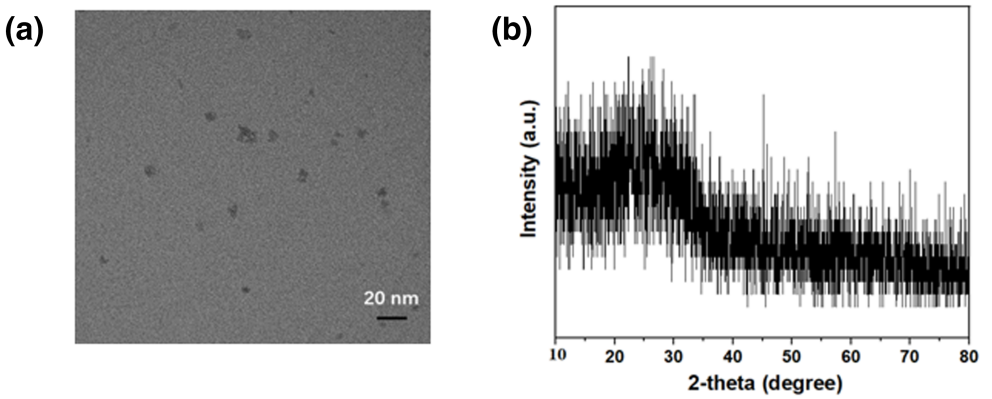

FIGURE 1 (a) TEM image, (b) XRD image, (c) FTIR spectra, and (d) UV–vis spectra of MoS_2 QDs

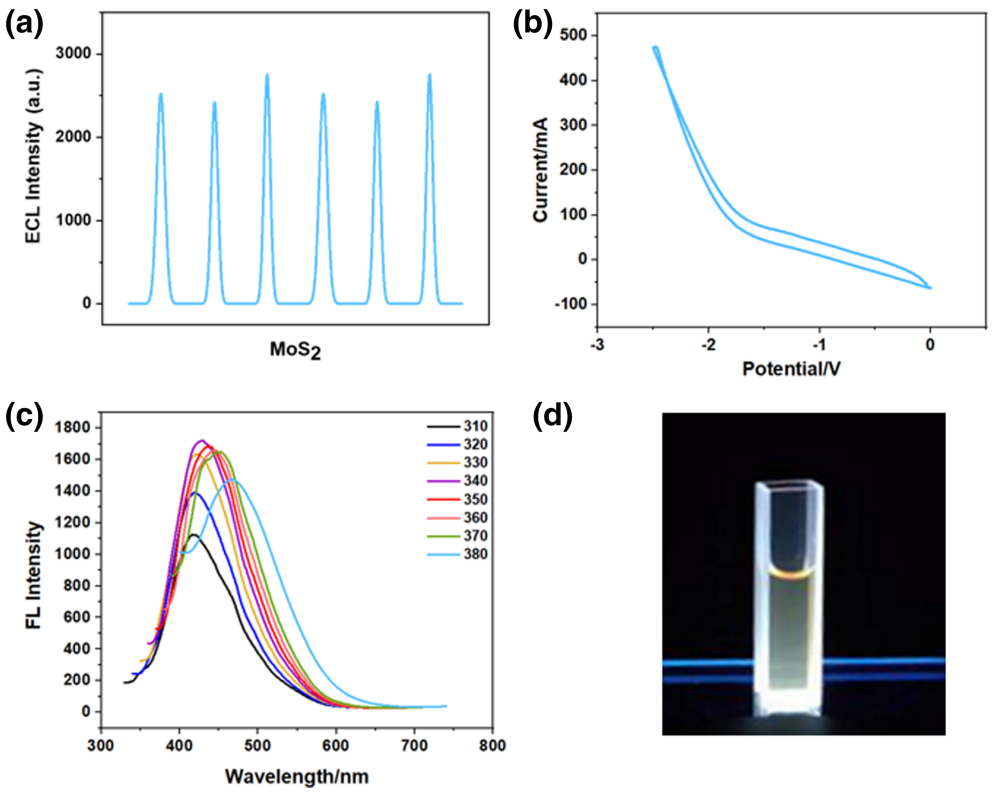

FIGURE 2 (a) ECL profiles and (b) cyclic voltammetry curve of MoS_2 QDs with 10 mmol/L H_2O_2 solution. (c) Photoluminescence spectrum and (d) the fluorescence photograph of MoS_2 QDs under a UV lamp

peaks observed at 3490 cm^{-1}, the existence of carboxyl groups can be inferred. Peaks at 1375 cm^{-1} corresponded to the stretching vibrations of C–O. These functional groups helped PLGA nanoparticles to load MoS_2 QDs and UAO molecules on the surface as nanosponge and were further embedded in the gel. SEM photographs of the nanosponge–hydrogel system are shown in Figure 3c. The structure

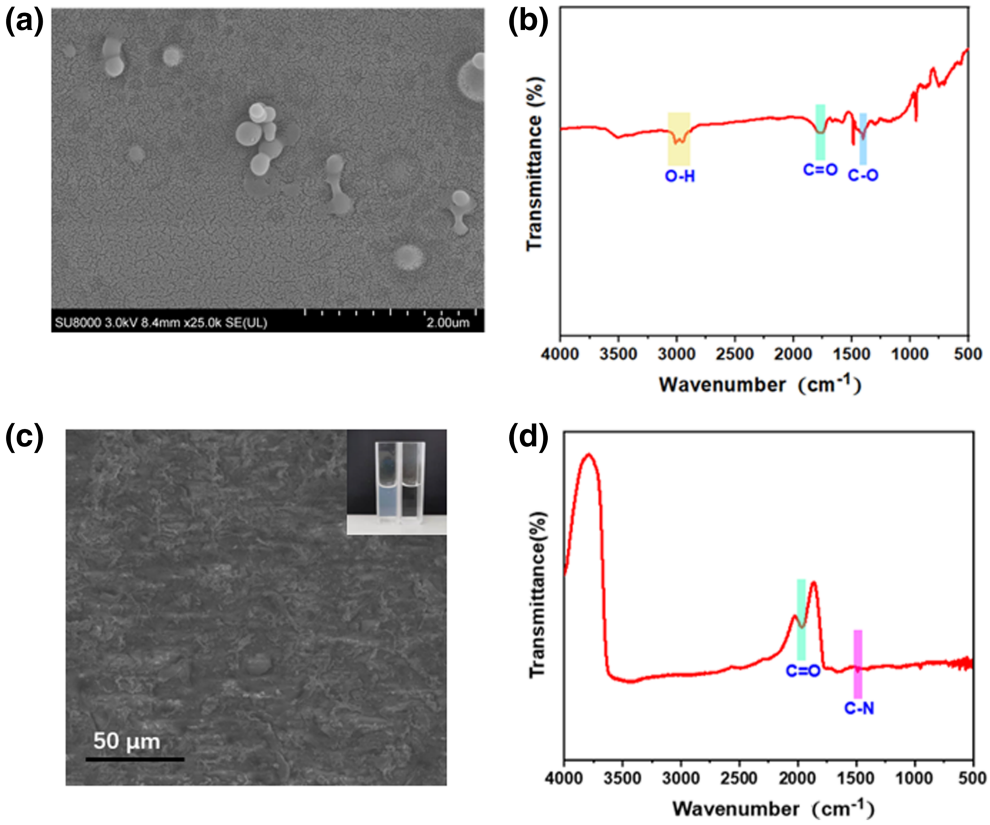

FIGURE 3 (a) SEM image and (b) FTIR spectra of PLGA nanoparticles. (c) SEM image of the nanosponge–hydrogel. Inset is a photograph of the nanosponge–hydrogel (left) and the hydrogel (right). (d) FTIR spectra of the nanosponge–hydrogel

of the gel was not closely linked, but had a loose structure with a defined gap. The structure provided an effective pathway for PLGA nanoparticles to adsorb UA molecules and then generate H_2O_2. As a result, ECL signals for MoS_2 QDs can be detected. The insert photograph in Figure 3c shows that the gel without the nanosponge–hydrogel was colourless and transparent. By contrast, the nanosponge–hydrogel system was an homogeneous milky white. This also confirmed that the PLGA nanoparticles had been dispersed evenly in the gel. FTIR spectroscopy of the nanosponge–hydrogel system is shown in Figure 3d. The characteristic peaks locating at 1950 cm^{-1} were attributed to the C=O bond. The peaks at 1500 cm^{-1} corresponded to the stretching vibrations of the C–N bond, which indicated the existence of amide bonds.

As seen in Figure 4a, cyclic voltammetry curves showed that the excitation potential of MoS_2 QDs was −1.8 V. When MoS_2 QDs were embedded into the nanosponge–hydrogel system, the changed reduction potential indicated the poor conductivity of the nanosponge–hydrogel. In addition, the ECL intensity of the MoS_2 QDs in the nanosponge–hydrogel system was approximately seven times higher than that of separated MoS_2 QDs (Figure 4b). This indicated that the nanosponge–hydrogel system can significantly promote the ECL of the MoS_2 QDs. The PLGA nanoparticles can work as carriers to load more QDs. Conversely, there were many ester groups and amide bonds in the nanosponge–hydrogel structure. Due to the large number of lone electron pairs, electrons can be excited in the ECL process to decrease the excitation potential. Electrochemical impedance spectroscopy (EIS) was investigated to characterize the impedance changes of the nanosponge–hydrogel system. As shown in Figure 4c, because of the poor conductivities of the gel and MoS_2 in this structure, the impedance value of the modified electrode increased largely with the bare electrode. It can be clearly observed that the impedance value increased gradually. Figure 4d shows the ECL response of the MoS_2 QDs and the nanosponge–hydrogel system with UA. When UA reacted with UAO in the buffer solution (pH 7.4) containing MoS_2 QDs, a significant ECL signal could be observed. This indicated that H_2O_2 was produced in the buffer solution due to catalysis of UAO, which further worked as a co-reactant to generate the ECL signal. There was also no obvious signal for the MoS_2 QDs in the nanosponge–hydrogel system without UA. When UA was absorbed into the nanosponge–hydrogel system, the ECL strength was greatly enhanced, and was five times higher than that of the MoS_2 QDs. The results confirmed the feasibility the nanosponge–hydrogel system-based ECL sensor for UA detection. The possible sensing mechanisms is as follows:

$$\mathrm{UA} + \mathrm{UAO@nanosponge-hydrogel} \rightarrow \mathrm{H_2O_2} \quad (4)$$

$$\mathrm{H_2O_2} + \mathrm{e^-} \rightarrow \cdot\mathrm{OH} + \mathrm{OH^-} \quad (5)$$

$$\cdot\mathrm{OH} + \mathrm{MoS_2\ QDs@nanosponge-hydrogel} + \mathrm{e^-} \rightarrow \mathrm{MoS_2\ QDs@nanosponge-hydrogel^*} + \mathrm{OH^-} \quad (6)$$

$$\mathrm{MoS_2\ QDs@nanosponge-hydrogel^*} \rightarrow \mathrm{MoS_2\ QDs@nanosponge-hydrogel} + \mathrm{hv} \quad (7)$$

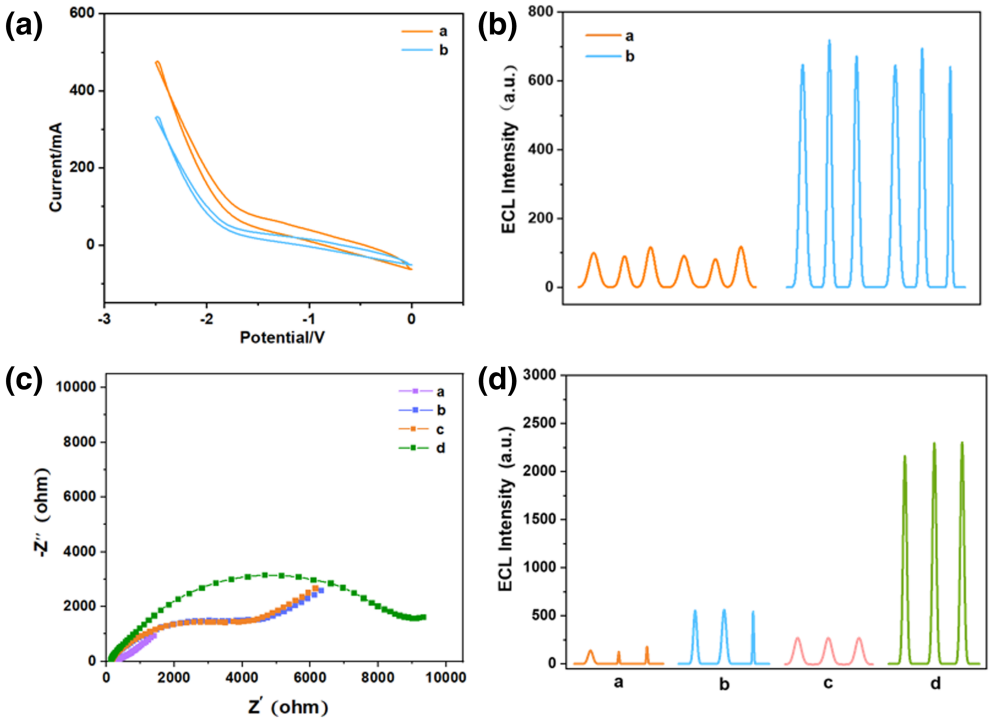

FIGURE 4 (a) Cyclic voltammetry curves and (b) ECL profiles of MoS_2 QDs (sample a) and MoS_2 QDs@nanosponge–hydrogel (sample b). (c) Electrochemical impedance spectroscopy of (sample a) bare electrode, (sample b) hydrogel, (sample c) PLGA nanoparticle–hydrogel, and (sample d) UAO@MoS_2 QDs@nanosponge–hydrogel. (d) ECL response of (sample a) bare electrode and (sample b) MoS_2 QDs with UAO/UA in PBS (pH 7.4). ECL response of UAO@ MoS_2 QDs @nanosponge–hydrogel without UA (sample c) and with UA (sample d)

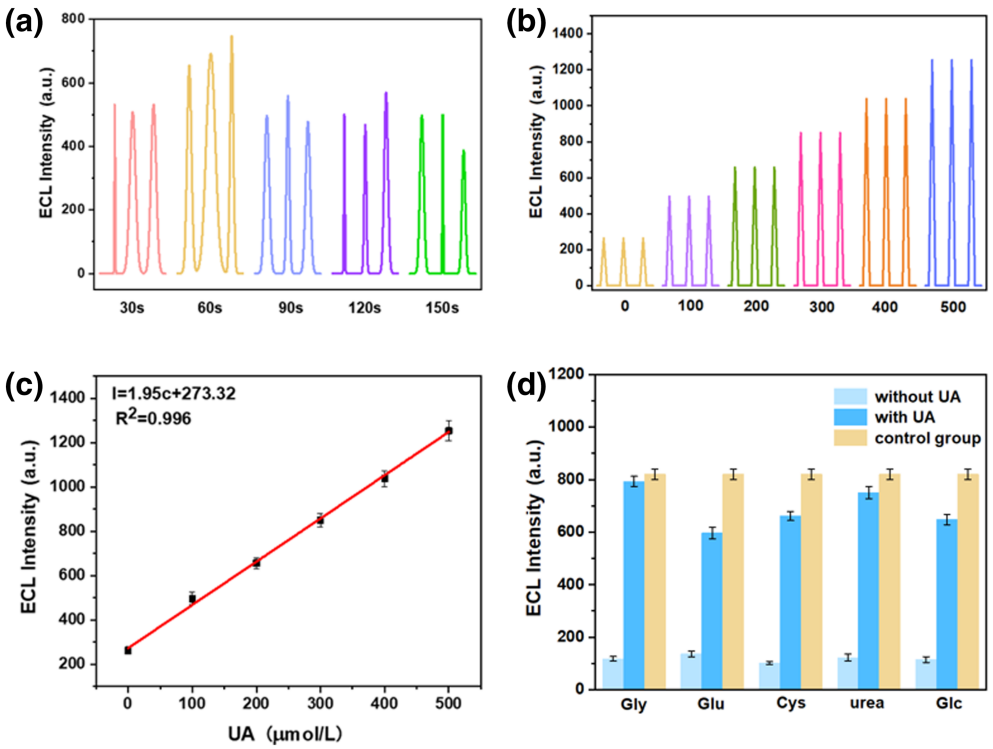

FIGURE 5 (a) ECL response of nanosponge–hydrogel with UA at different reaction times. (b) Relationship between the ECL intensity and the different concentrations of UA (μmol/L). (c) Corresponding linear relationship for UA detection. (d) Selectivity of the ECL sensor. The concentration of UA was 300 μmol/L, the concentrations of Gly, Glu, Cys, urea and Glu were 5 mg/ml

3.3 | Analytical performance of the nanosponge–hydrogel system-based biosensor

The sensing time of the nanosponge–hydrogel system was investigated and shown in Figure 5a. The ECL intensity reached maximum at 60 s. The detection speed was fast and suitable for a point of care test. Therefore, the reaction time was chosen as 60 s. Based on the nanosponge–hydrogel system, a series of different concentrations of UA was detected under the ECL response of the MoS_2 QDs. ECL intensity was enhanced with increasing concentrations of UA from 100 to 500 μmol/L. A good linear relationship between ECL intensity and concentration was observed and shown in Figure 5c. The linear regression equation was $I = 1.95c + 273.32$ ($R^2 = 0.996$) with a limit of detection (LOD) at 0 μmol/L. To evaluate the selectivity of the

TABLE 1 Determination of UA in clinical serum samples

Number	UA (sample) (μmol/L)	UA (standard) (μmol/L)	UA (all) (μmol/L)	Recovery (%)	RSD (%)
1	150.1	300.0	222.4	98.3	3.2
2	248.6	300.0	285.0	107.1	4.6
3	163.9	300.0	224.5	95.0	2.7

TABLE 2 Comparison of the analytical methods for UA detection

Determine method	Materials	Linear range (μM)	LOD (μM)	Reference
Spectrophotometry	Fe-Phen	2.97–23.8	0.71	[20]
SERS	Ag NP_S	5–1000	5	[21]
Fluorescence	CDS QD_S	125–1000	125	[22]
ECL	CNCo/GCE	2–100	0.83	[23]
ECL	Nanosponge–hydrogel	100–500	30	This work

nanosponge–hydrogel system, glycine, glutamate, cysteine, urea, and glucose were added as interferences under the same experimental conditions. The results in Figure 5d show that the ECL signal of these interfering substances was quite low. It can be observed that the ECL intensity decreased with cysteine or glucose due to their strong reducing ability. Because of the nanosponge structure, MoS_2 QDs, and UAO were immobilized together on the PLGA nanoparticles. Therefore, most H_2O_2 generated from urate oxidase can react with QDs directly. This can effectively overcome the interference from cysteine or glucose. Moreover, the concentration of cysteine or glucose in the experiment was 5 mg/ml, which is less than is present in the human body (0.702–1.404 mg/ml). The ECL intensity significantly enhanced only with the addition of UA, which demonstrated that the ECL biosensor was reliable and with a satisfactory anti-interference ability. To further demonstrate the practicability of the ECL sensing system, UA was detected in clinical serum samples. The detection results are listed in Table 1. The UA concentrations in the serum from the three samples were 150.1 μmol/L, 248.6 μmol/L, and 163.9 μmol/L. The normal UA content in men is 150–350 μmol/L and in women is 100–300 μmol/L,[19] therefore the UA content of the three samples was in the normal range. The recoveries were acceptable at between 95.03% and 107.13%. Compared with previously reported assays for UA detection shown in Table 2, this ECL method has an appropriate linear range and low detection limit. In addition, the method has good sensitivity, certain reliability, a simple detection method, and has a certain application prospect in clinical diagnosis.

4 | CONCLUSION

In conclusion, we developed a novel ECL biosensor based on the nanosponge–hydrogel system to detect UA. UAO on the PLGA nanoparticles can catalyze UA to product H_2O_2 *in situ*, which further reacts with MoS_2 QDs and generates an ECL signal. The nanosponge–hydrogel system possessed a large loading capability for biomolecules and nanoparticles. Furthermore, the biosensor showed a significant adsorption function, structural integrity, modification flexibility, and ECL amplification. The ECL sensing system provides a new sensing strategy for the detection of UA content in clinical diagnosis. This ECL sensor is nontoxic and harmless, and shows a potential function as a wearable sensor. Although there are still some important issues to be solved in further study, the nanosponge–hydrogel system does provide a new sensing pathway.

ACKNOWLEDGEMENTS

The present work was supported by the science research project (No. JJKH20211050KJ) in the Education Department of Jilin Province, China.

STATEMENT ON ETHICAL APPROVAL

The use of human serum samples was approved by the ethics committee of the China–Japan Union Hospital of Jilin University (No. 2021-KYLY-020016).

ORCID

Qiang Ma https://orcid.org/0000-0002-9193-9341

REFERENCES

[1] T. Han, M. Wang, W. Li, M. An, H. Fu, *J. Biomed. Nanotechnol.* **2021**, *17*, 2071.
[2] D. Luis-Rodríguez, J. Donate-Correa, E. Martín-Núñez, C. Ferri, V. G. Tagua, A. P. Castro, C. Mora-Fernández, J. F. Navarro-González, *Rheumatology* **2021**, *60*, 371.
[3] M. Marin, N. Maalouf, *J. Invest. Med.* **2018**, *66*, 1031.
[4] H. Khajehsharifi, H. Tavallali, M. Shekoohi, M. Sadeghi, *Drug Test. Anal.* **2013**, *5*, 353.
[5] H. Chu, X. Wei, M. Wu, J. Yan, Y. Tu, *Sens, Actuator. B-Chem.* **2012**, *163*, 247.
[6] J. Ren, W. Yang, X. Niu, J. Gao, *Chinese J. Chem.* **2012**, *30*, 288.
[7] M. Amjadi, E. Rahimpour, *Microchim. Acta* **2012**, *178*, 373.
[8] Q. Hu, J. Yang, Z. Zheng, Y. Ding, Y. Chen, W. Gao, *Biosens. Bioelectron.* **2019**, *143*, 11627.
[9] Z. Liu, L. Wang, P. Liu, K. Zhao, S. Ye, G. Liang, *Food Chem.* **2021**, *357*, 129753.
[10] P. Chansri, Y. Sung, *Surf. Coat. Technol.* **2016**, *294*, 220.
[11] J. H. Kwon, Y. M. Kim, H. C. Moon, *ACS Nano* **2021**, *15*, 15132.

[12] L. Zong, L. Ruan, J. Li, R. S. Marks, J. Wang, S. Cosnier, X. Zhang, D. Shan, *Biosens. Bioelectron.* **2021**, *184*, 113216.
[13] F. Wang, W. Gao, S. Thamphiwatana, B. T. Luk, P. Angsantikul, Q. Zhang, C. M. Hu, R. H. Fang, J. A. Copp, D. Pornpattananangkul, W. Lu, *Adv. Mater.* **2015**, *27*, 3437.
[14] X. Wang, Y. Zhang, W. Xue, H. Wang, X. Qiu, Z. Liu, *J. Biomater. Appl.* **2017**, *31*, 923.
[15] I. Serris, P. Serris, K. M. Frey, H. Cho, *AAPS PharmSciTech* **2020**, *21*, 256.
[16] M. Zhang, Y. Liao, X. Tong, F. Yan, *RSC Adv.* **2022**, *12*, 4072.
[17] Y. Jiao, Y. Xing, K. Li, Z. Li, G. Zhao, *Luminescence* **2021**, *36*, 1110.
[18] Y. Nie, Y. Liu, Q. Zhang, F. Zhang, Q. Ma, X. Su, *Anal. Chim. Acta* **2020**, *29*, 190.
[19] L. Jin, T. Zhu, L. Xu, W. Zhang, B. Liu, C. Jiang, H. Yu, L. Huang, K. KeungCheng, G. NeilThomas, T. HingLam, *Int. J. Cardiol.* **2013**, *168*, 2238.
[20] S. Boroumand, M. A. Chamjangali, G. Bagherian, *Spectrochim. Acta a* **2017**, *174*, 203.
[21] Y. Lu, C. Wu, R. You, Y. Wu, H. Shen, *Biomed. Opt.* **2018**, *9*, 4988.
[22] N. E. Azmi, N. I. Ramli, J. Abdullah, M. A. Abdul Hamid, *Biosens. Bioelectron.* **2015**, *67*, 129.
[23] L. Liu, L. Liu, Y. Wang, *Talanta* **2019**, *199*, 478.

How to cite this article: W. Liu, Y. Nie, M. Zhang, K. Yan, M. Wang, Y. Guo, Q. Ma, *Luminescence* **2022**, *37*(9), 1524. https://doi.org/10.1002/bio.4326